Hedamycin intercalates the DNA helix and, through carbohydrate-mediated recognition in the minor groove, directs N7-alkylation of guanine in the major groove in a sequence-specific manner

Mark Hansen, Sang Yun and Laurence Hurley*

Drug Dynamics Institute, College of Pharmacy, The University of Texas at Austin, Austin, TX 78712-1074, USA

Background: The pluramycins are a class of antitumor antibiotics that exert their biological activity through interaction with DNA. Recent studies with the analog altromycin B have determined that these agents intercalate into the DNA molecule, position carbohydrate substituents into both major and minor grooves, and alkylate the DNA molecule by epoxide-mediated electrophilic attack on N7 of guanine located to the 3' side of the drug molecule. Alkylation is sequence dependent and appears to be modulated by glycoside substituents attached at the corners of a planar chromophore. The altromycin B-like analogs preferentially alkylate 5'AG sequences; hedamycin-like analogs prefer 5'TG and 5'CG sequences. Although the mechanism of guanine modification by altromycin B has been extensively studied, the mechanism of action of hedamycin has not been previously determined.

Results: Using high-field NMR, we have shown that hedamycin stacks to the 5' side of the guanine nucleotide at the site of intercalation in a DNA decamer, positioning both aminosaccharides into the minor groove to direct alkylation by the epoxide moiety on N7 of guanine. The C10 linked N,N-dimethylvancosamine sugar moiety interacts to the 5' side of the intercalation site, while the C8 linked anglosamine moiety interacts to the 3' side. The binding interactions of the two aminosugars steer the C2 double epoxide located in the major groove into the proximity of N7 of guanine. Unexpectedly, it is not the first epoxide that undergoes electrophilic addition to N7 of guanine, which would correspond to altromycin B, but the second, terminal epoxide.

Conclusions: We have used two-dimensional NMR to elucidate the sequence-selective recognition of DNA by hedamycin and the mechanism of covalent modification of guanine by this antibiotic. Characterization of the intermolecular interactions between both hedamycin and altromycin B and their targeted DNA sequences has yielded a better understanding of the reasons for variations in sequence selectivity and alkylation reactivity among the pluramycin compounds.

Chemistry & Biology April 1995, **2**:229–240

Key words: DNA recognition, hedamycin, pluramycins, NMR

Introduction

Hedamycin and altromycin B are two of the most biologically potent and structurally complex natural products of the pluramycin family of antitumor antibiotics (Fig. 1). Extensive studies of the pluramycin analog, altromycin B, have clearly shown that this family of antibiotics achieves activity by intercalating and alkylating the DNA molecule [1,2]. Structurally, hedamycin and altromycin B represent two distinct subgroups within the pluramycin family, namely the classical pluramycins and the altromycins. Although bearing identical 4H-anthra[1,2-b]pyran-4,7,12-trione chromophores, the subgroups differ structurally in the attached substituents at the C2, C5, C8, and C10 positions [3–12]. These differences translate into variations in biochemical activity, that is, alkylation reactivity and sequence selectivity [13]. Both subgroups require a C2 epoxide functionality for high cytotoxic activity as well as for DNA alkylation through N7 of guanine [5]. The classical pluramycins, represented by hedamycin, bear two aminosugars, an anglosamine attached to the C8 position and an N,N-dimethylvancosamine attached to the C10 position. Various substituents can be found at the C2 position among members of this subgroup, including a vinyl substituent (kidamycin) [14–16], a vinylepoxide (pluramycin A) [17,18], a single epoxide (epoxykidamycin) [19], or a double epoxide (hedamycin) [20–22]. The altromycins, on the other hand, bear an aminodisaccharide on the C10 position, an invariant single epoxide at the C2 position, and in many cases (altromycin B), a methyl ester-linked 6-deoxy-3-O-methylaltrose attached through the C5 position [23–25].

Recent investigations into the interaction between altromycin B and DNA have revealed a general mode of DNA interaction for the pluramycins as a group and have indicated possible roles for the C5, C8 and C10 linked glycosidic functionalities in DNA sequence recognition [1,2]. These recent studies clearly demonstrate that altromycin B threads the DNA molecule, intercalates to the 5' side of the modified guanine, and positions a neutral altrose moiety in the major groove and an aminodisaccharide in the minor groove. Thus positioned,

*Corresponding author.

 ISSN 1074-5521

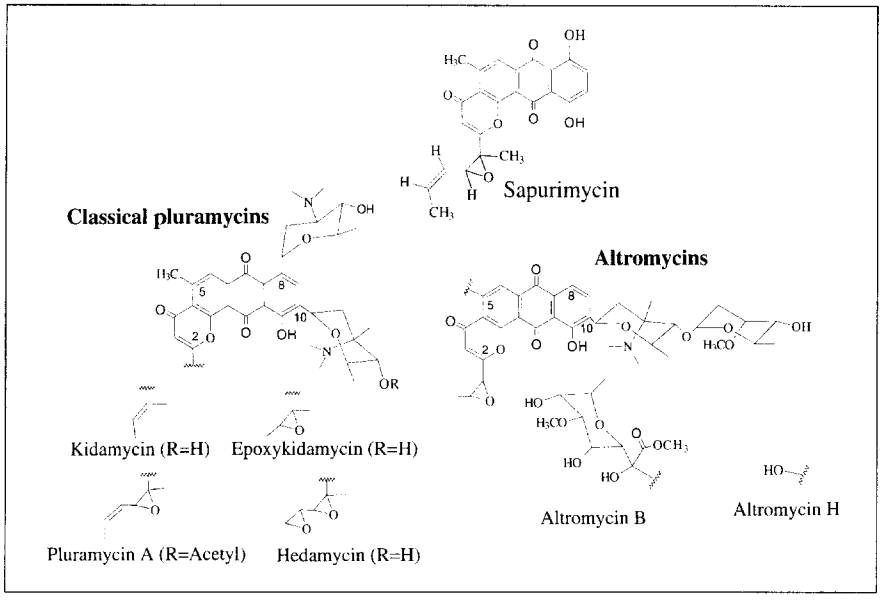

Fig. 1. Structures of representative pluramycin antibiotics. The family subdivides by structure into two distinct groups: the classical pluramycins (depicted by kidamycin, epoxykidamycin, pluramycin A, and hedamycin) and the newly discovered altromycins (depicted by altromycins B and H). Sapurimycin represents the simplest pluramycin analog.

altromycin B alkylates DNA through N7 of guanine in the major groove by electrophilic attack by the epoxide attached to the C2 position of the tetracyclic chromophore. To decipher the functional significance of the different structural motifs displayed by the classical pluramycins and the altromycins, namely the C2, C5, C8 and C10 substituents, the contrasting pluramycin analog, hedamycin, has been reacted with the $[d(GA\underline{TG}\star TACATC)]_2$ ($\star$ denotes site of covalent modification and underlined is the site of intercalation) duplex to form a bis-adduct (Fig. 2). Resolving the molecular interactions that hedamycin makes with DNA provides a basis for understanding hedamycin's demonstrated 5'(Py)G$\star$ (Py = pyrimidine) alkylation selectivity [13], the functional importance of the second, terminal epoxide, and the increased alkylation reactivity demonstrated by hedamycin over the altromycins.

Although hedamycin alkylates N7 of guanine in a fashion similar to altromycin B, it does so through C18 of the terminal epoxide as opposed to the equivalent site (C16) through which altromycin B alkylates guanine. Like altromycin B, hedamycin also intercalates the DNA molecule and stacks to the 5' side of the modified guanine, thereby positioning both the C8 and C10 aminosaccharides for interaction in the minor groove. Hedamycin achieves its 5'(Py)G$\star$ sequence selectivity through interactions between the two aminosugars and the O2 carbonyl of pyrimidines located in the minor groove.

Results

Due to the serious stability limitations of guanine N7-alkyl adducts [2,26] (C. Lin & D.J. Patel, personal communication), a noncovalent classical pluramycin analog was first chosen for NMR studies. The $[d(GATGTACATC)]_2$ decamer duplex was initially reacted with the noncovalent analog kidamycin. As the ligand was titrated into the DNA duplex sample, analysis of one-dimensional NMR spectra revealed general broadening of the proton spectrum, indicative of non-specific interaction with the DNA molecule. Subsequently, an identical DNA sample was reacted with two equivalents of the analog hedamycin, in which the C2 vinyl functionality of kidamycin is replaced with a reactive double epoxide. The addition of 2:1 molar equivalents of hedamycin to the 10 base-pair DNA duplex yielded a C2 symmetric diadduct that exhibited nine methyl resonances. Samples proved to be marginally more stable than the previously studied altromycin B diadducts, but degraded similarly into a complex mixture of products over the span of four to five days. Samples also displayed a high degree of aggregation and had to be diluted to diminish line broadening at the expense of signal intensity. For similar reasons, acquisition of data was carried out at 30 °C, which also minimized problems with aggregation.

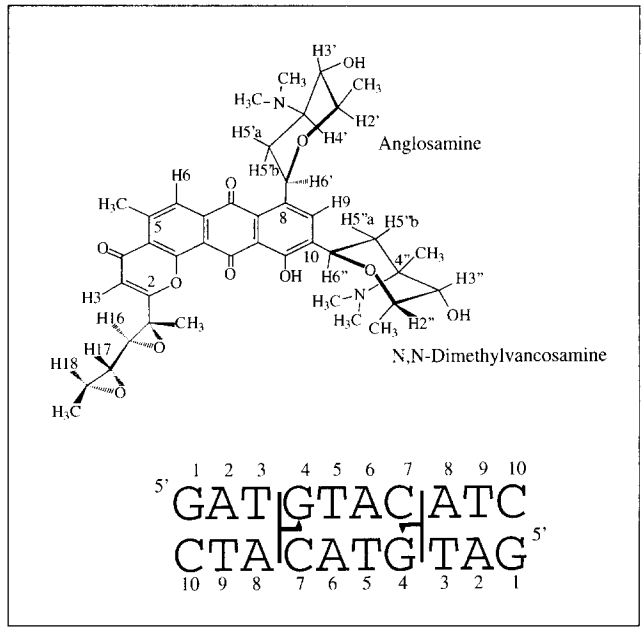

Fig. 2. The structures and numbering schemes of hedamycin and the DNA decamer used in this study. Shown are sites of intercalation between 3T and 4G and covalent modification (4G).

Assignment of the hedamycin proton resonances

The hedamycin proton resonances (Table 1) are divided into four regions of the hedamycin molecule: the aromatic chromophore, the C8 linked anglosamine, the C10 linked N,N-dimethylvancosamine and the C2 double epoxide. Protons in each region were assigned using total correlation spectroscopy (TOCSY), double quantum filtered correlation spectroscopy (DQF-COSY) and nuclear Overhauser effect spectroscopy (NOESY) NMR experiments [27–30]. In the first group of resonances, those attached directly to the intercalating chromophore, the H9 resonance was identified by NOESY connectivities to the H2', 2' methyl and 4" methyl located on the aminosugars attached to the C8 and C10 positions. The 5 methyl (singlet) and the adjacent H6 proton were assigned based on a NOESY connectivity to each other and a weak contact between the 5 methyl and H3 resonances. The H3 proton resonance was easily assigned based on NOESY connectivities to resonances associated with the C2 epoxide arm.

In the C8 linked anglosamine (designated in single-prime numbers), the proton resonances mutually coupled around the sugar ring in the DQF-COSY. Couplings between H6' and H5'a, H6' and H5'b, H5'b and H4', H4' and H3', and H3' and H2' establish these proton assignments. The 2' methyl resonance (doublet) was easily identified through coupling to the H2'. The 4' dimethylamino signal was identified by resonance intensity, chemical shift, and NOESY connectivities to the other protons on this sugar. The H5'a and H5'b resonances were distinguished based on stronger NOE connectivities between the H5'b to the H6' and H4' protons than the equivalent NOEs for the H5'a resonance.

In the C10 linked N,N-dimethylvancosamine moiety (designated with double-prime numbers), the 4" dimethylamino signal is easily identified by chemical shift, one-dimensional intensity, and strong NOESY contact to the 4" methyl resonance (singlet). H5"a and H5"b protons both showed NOESY contacts to the 4" methyl and 4" dimethylamino signals. Additionally, the H5"a proton couples with both the H5"b and the H6" protons. The 2" methyl (doublet) coupled to the H2" and showed NOE contacts to both 4" substituents. The H3" proton was assigned based on NOESY connectivities to both the 4" and 2" methyl and proton resonances. The proton assignments of H5"b and H5"a were distinguished based on correlation of their chemical shifts to that of the free drug and a stronger NOE connectivity between the 4" methyl to the H5"b than between the 4" methyl to the H5"a resonance.

Proton resonances in the last group associated with the site of covalent attachment of the drug to the DNA were assigned through mutual couplings between vicinal protons on the C2 epoxide arm (Fig. 3). The H16 coupled in the DQF-COSY to the H17 resonance, which in turn coupled to the H18 proton. The H18 similarly coupled to the terminal 19 methyl (doublet). The 15 methyl (singlet) was assigned by NOESY contacts to the H3, H16, H17 and H18 protons. Carbon-13 chemical shifts for the backbone of the C2 epoxide arm were identified through single-bond and multiple-bond ^{1}H–^{13}C correlations to the previously identified proton resonances. The C15, C16, C17, C18 and C19 resonances were all assigned through coupling to their respective attached proton resonance, and the C14 resonance was assigned based on long-range coupling to the 15 methyl.

Table 1. Comparison of the hedamycin chemical shifts in the bis-hedamycin–[d(GATGTACATC)]$_2$ diadduct and the free drug.

	Chemical shifts (ppm) of hedamycin	
^{1}H assignment[a]	in the bis-adduct[b]	free drug[c]
H3	6.16	6.46
H6	6.36	8.00
5CH_3	2.33	2.99
H9	8.22	8.33
15CH_3	1.08	1.96
H16	3.34	3.32
H17	3.78	2.89
H18	5.09	3.11
19CH_3	1.73	1.44
H2'	3.94	3.55
2'CH_3	1.57	1.43
H3'	3.38	3.19
4'N(CH_3)$_2$	2.73	2.32
H4'	3.50	2.93
H5'a	1.05	1.20
H5'b	1.80	2.50
H6'	5.39	5.45
H2"	4.32	4.04
2"CH_3	1.48	1.51
H3"	3.78	3.35
4"CH_3	1.16	0.71
4"N(CH_3)$_2$	2.90	2.22
H5"a	2.58	2.10
H5"b	3.00	2.70
H6"	5.57	5.45

[a]For numbering, see Figure 2.
[b]Chemical shifts referenced to H_2O in 99.9 % D_2O.
[c]Chemical shifts in chloroform [5,22].

Assignments of DNA proton resonances

DNA proton assignments of the 10 base-pair duplex and its bis-hedamycin diadduct (Table 2) were achieved through established methods [31] using TOCSY, NOESY and DQF-COSY experiments to create walks leading from the 5' end to the 3' end of the DNA molecule (Fig. 4). To identify protons overlapping the water resonance, namely the 5TH3' and the 4GH3' resonances, a 150 ms NOESY experiment was collected at 40 °C, which shifted these resonances slightly downfield of the water resonance. The aromatic to aromatic, aromatic to H1', aromatic to H2'/2", and aromatic to H3' resonances all demonstrate breaks in the walks at the 3T–4G and 7C–8T steps due to insertion of the intercalating chromophore at this position on the DNA molecule. Interestingly, the 5TH1' resonance is upfield shifted from 5.71 ppm to 5.17 ppm upon hedamycin–duplex adduct formation, presumably due to

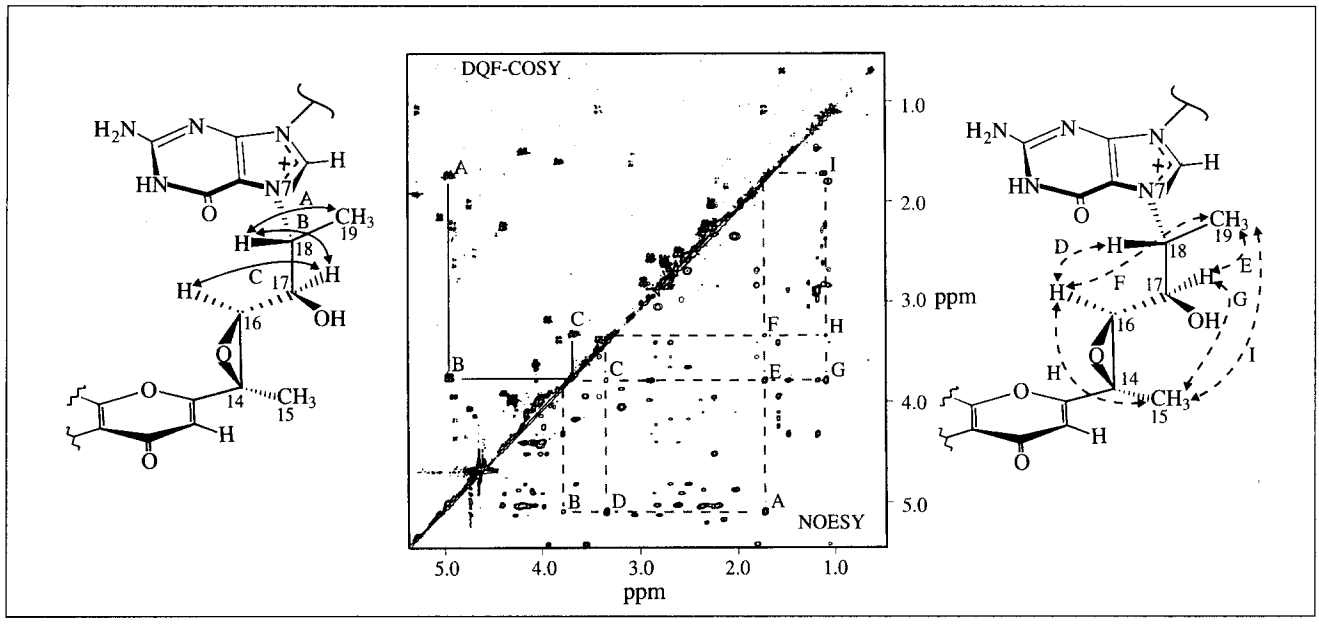

Fig. 3. Assignments for the proton resonances associated with the reacted C2 double-epoxide substituent. A DQF-COSY experiment is shown left of the diagonal with a corresponding chemical structure in which couplings between H18 and 19 methyl (A), H18 and H17 (B), and H16 and H17 (C) are identified. A NOESY experiment (150 ms mixing time) is shown right of the diagonal with a corresponding chemical structure showing cross-peaks between H18 and H16 (D), H17 and 19 methyl (E), H16 and 19 methyl (F), H17 and 15 methyl (G), H16 and 15 methyl (H), and 19 methyl and 15 methyl (I).

its proximity to the aromatic system of the drug, which extends into the minor groove.

C18 of hedamycin alkylates N7 of guanine via an S_N2 mechanism

Both the base and the site of covalent attachment to the DNA molecule are identified by the chemical nature of the 4GH8 aromatic proton. This proton, which was identified and characterized in 95 % H_2O, has become extremely labile and now resonates at 9.6 ppm, which is ~2 ppm downfield of the equivalent proton resonance in the unmodified 10 base-pair duplex (7.77 ppm). The unusually acidic nature of this H8 aromatic proton is a direct result of alkylation that occurs through N7 of guanine, thereby forming a cationic drug–guanine lesion. These results are consistent with other reported N7 alkyl-guanine adducts, specifically aflatoxin, sapurimycin and altromycin B [2,26] (C. Lin & D.J. Patel, personal communication).

In comparison to the unreacted C2 double epoxide functionality of hedamycin, the H18 and C18 demonstrate the greatest change in chemical shift upon DNA adduct formation, ~2 and 20 ppm downfield, respectively, whereas H17 and C17 demonstrate only marginal downfield shifts of ~1 and 14 ppm, respectively (Fig. 5, Table 3). The resonances associated with the C14–C16 epoxide demonstrate only small chemical shift differences over the free drug. It is therefore proposed, based

Table 2. Comparison of the DNA proton chemical shifts[a] of the bis-hedamycin–[d(GATG*TACATC)]$_2$ duplex diadduct with the unmodified duplex.

Base	H8/H6	H5/5CH$_3$	H2	H1'	H2'	H2"	H3'	H4'
1G	7.85 (0.00)	–	–	5.58 (–0.07)	2.52 (–0.04)	2.70 (–0.05)	4.83 (–0.02)	4.12 (–0.07)
2A	8.20 (–0.13)	–	7.88 (–0.07)	6.18 (–0.13)	2.60 (–0.15)	2.85 (–0.13)	5.03 (0.00)	4.40 (–0.07)
3T	7.30 (+0.15)	**1.12 (–0.30)**	–	**6.10 (+0.31)**	2.25 (+0.13)	2.38 (–0.09)	5.00 (+0.14)	**4.42 (–0.29)**
4G*	**9.60 (+1.80)**[b]	–	–	5.82 (–0.11)	2.32 (–0.25)	**2.47 (–0.28)**	4.75 (–0.18)	4.45 (+0.07)
5T	7.10 (–0.10)	**1.13 (–0.24)**	–	**5.18 (–0.52)**	2.15 (+0.07)	**2.15 (–0.31)**	4.75 (–0.12)	**3.87 (–0.43)**
6A	8.20 (–0.03)	–	7.50 (+0.08)	6.11 (–0.07)	2.60 (–0.06)	2.82 (+0.01)	4.92 (–0.09)	4.40 (0.00)
7C	7.34 (+0.14)	5.20 (–0.10)	–	**5.68 (–0.34)**	2.20 (+0.15)	2.34 (–0.03)	**5.04 (+0.24)**	4.24 (0.00)
8A	**8.62 (+0.42)**	–	**6.88 (–0.25)**	6.40 (–0.19)	2.81 (+0.19)	3.05 (+0.17)	5.13 (+0.18)	4.20 (–0.18)
9T	7.10 (–0.12)	1.27 (–0.17)	–	5.86 (–0.17)	2.03 (–0.02)	2.36 (–0.10)	4.88 (+0.04)	**4.14 (–0.24)**
10C	7.45 (–0.15)	5.52 (–0.18)	–	6.18 (–0.17)	2.25 (0.00)	2.25 (0.00)	4.52 (–0.03)	**4.19 (–0.21)**

[a]Referenced to H_2O in 99.9 % D_2O unless otherwise noted. Chemical shift differences: (–) and (+) represent upfield and downfield shifts, respectively. Shown in bold are those greater than 0.2 ppm.
[b]Exchangeable proton observed in 95 % H_2O.
*Site of covalent modification by hedamycin.

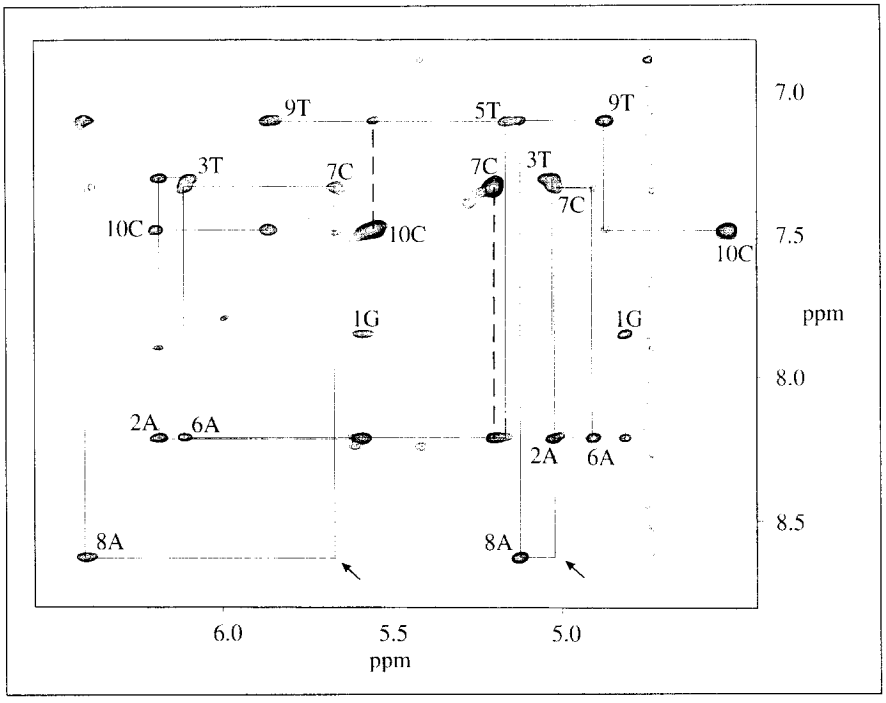

Fig. 4. NOESY data (150 ms) showing the aromatic to H1' (left) and aromatic to H3' walks (right). The intra-residue connectivities are identified with a base and number designation. Breaks in the walks due to ligand intercalation are indicated with arrows. Also shown are cytosine H5 connectivities to their own H6 proton and the 5' neighbor's aromatic proton. For 7C and 10C, these are shown by a single, broken vertical line. Note that cross-peaks associated with 4GH8 are absent due to the rapid exchange of this proton with D_2O.

on chemical shifts and chemical shift changes, that N7 of guanine performs nucleophilic attack on C18, leading to opening of the epoxide to form a hydroxyl on C17 (Fig. 6). Medium to strong NOEs between 4GH8 and both hedamycin H18 and H17, and only a medium to weak NOE between 4GH8 and hedamycin H16, also strongly argue for alkylation at C18. The relatively undisturbed chemical shifts of C14 and C16 suggest that the first, proximal epoxide associated with these two carbon atoms is chemically unmodified in the DNA adduct.

Alkylation of the duplex oligomer yields only one set of proton resonances corresponding to a single species of adduct. This suggests that nucleophilic addition occurs through an S_N2 mechanism, inverting the stereoconfiguration of the C18 chiral center. The stereochemistry reported in the crystal structure of hedamycin (14R, 16S, 17R, 18S) [20] would then be converted to 14R, 16S, 17R, 18R by an S_N2 nucleophilic addition to N7 of guanine. This stereochemical configuration (see Fig. 3) is supported by a strong NOE connectivity between hedamycin H18 and H16, a weaker NOE connectivity between H16 and H17 (medium), and strong NOEs between 15 methyl and 19 methyl, 15 methyl and 4GH8, and 19 methyl and 4GH8.

Drug–DNA connectivities in the major groove

The C2 substituent is located in the major-groove side of the DNA helix and is positioned next to the covalently modified strand, making NOESY contacts to both sides of the intercalation site (Fig. 7), confirming the site of intercalation. On the 5' side of the intercalation site, the 3T methyl shows NOE contacts to hedamycin H16; 3TH6, 3TH2', and 3TH2" show NOE contacts with hedamycin's 15 methyl. On the 3' side of the intercalation site, the 4GH8 and the 5T methyl show NOE contacts to the 19 methyl and H18 of hedamycin. Also in this region of the duplex is the H3 resonance of hedamycin, which shows a medium cross-peak to the 3T methyl of the DNA.

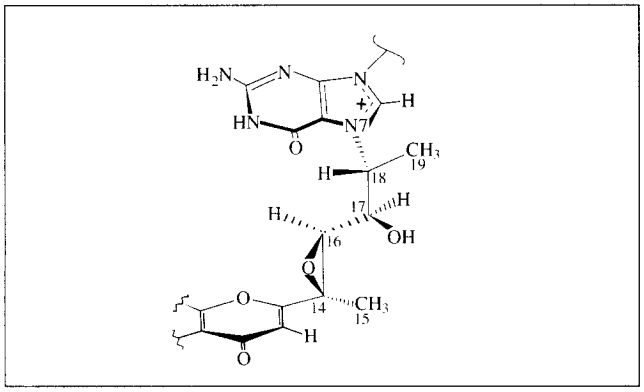

Fig. 5. Structure of the hedamycin C2 epoxide arm. Based on chemical shifs and chemical-shift differences (Table 3), it is C18 of the second epoxide that reacts with N7 of guanine.

Table 3. ^1H and ^{13}C NMR chemical shifts (ppm) of the C2 side chain of hedamycin as the free drug and after reaction with the 10 base-pair duplex DNA[a].

$^1H/^{13}C$ Assignment	^1H	^{13}C
14	— [b]	58.0 (+0.0)
15	1.1 (0.0)	14.0 (–0.1)
16	3.3 (0.0)	68.5 (+4.6)
17	**3.8 (+0.9)**[c]	**69.0 (+13.6)**
18	**5.1 (+2.0)**	**78.7 (+23.3)**
19	1.7 (+0.3)	15.6 (–1.6)

[a]Chemical shift differences are reported in parenthesis: DNA adduct in D_2O minus hedamycin in $CDCl_3$ [5,6,22]
[b]Not applicable.
[c]Chemical shifts experiencing significant downfield shifts upon reaction with DNA are designated in bold.

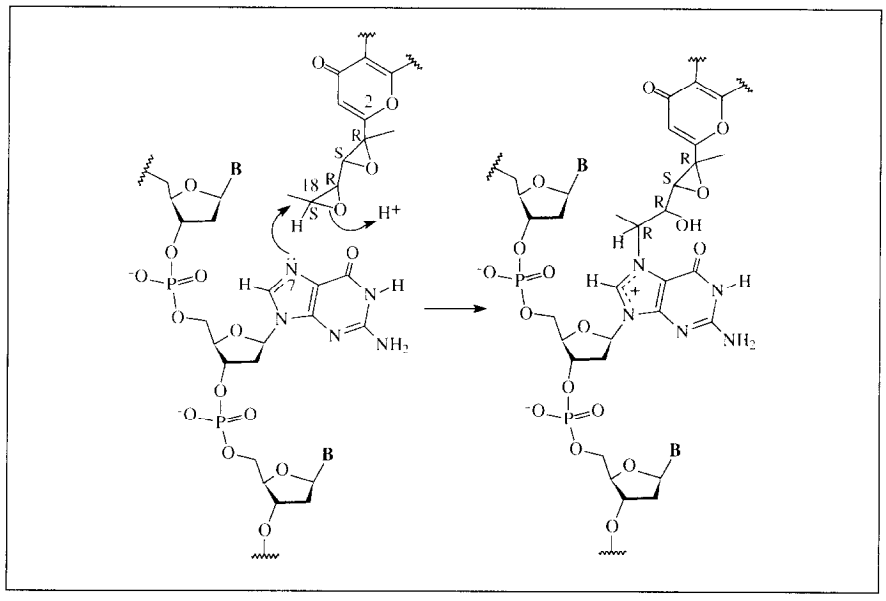

Fig. 6. The proposed mechanism of covalent modification of DNA by hedamycin. N7 of guanine performs nucleophilic attack on the terminal epoxide, forming a cationic lesion on the DNA. Subsequent depurination of the modified guanine results in DNA strand breakage [1].

Adjacent to the noncovalently modified strand in the major groove is the 5 methyl of the drug, which also shows contacts to both sides of the intercalation site. The 5 methyl shows medium connectivities to 7CH6 and 7CH5 and a very weak connectivity to 8AH8, all of which are located in the DNA major groove. Located between the grooves is the hedamycin H6 proton, which shows weak contact to the major groove proton 7CH6 and both a strong and a weak connectivity to 7CH1' and 7CH3', located in the minor groove. A diagrammatic summary of these intermolecular connectivities in the major groove is shown in Figure 7.

Drug–DNA connectivities in the minor groove

Both the C8 linked anglosamine and the C10 linked N,N-dimethylvancosamine are located in the minor groove of the DNA molecule (Fig. 8a). The NOE

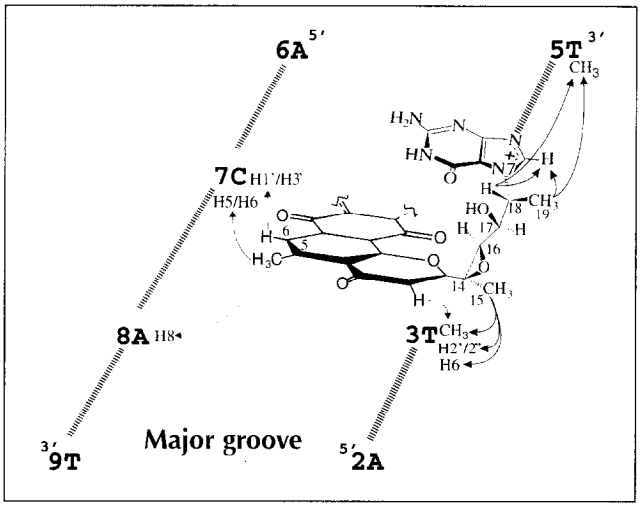

Fig. 7. Summary of key ^{1}H-NOESY connectivities (150 ms) between hedamycin and the DNA major groove. The drug shows connectivities to both sides of the intercalation site, reaffirming positioning of the tetracyclic chromophore between 3T and 4G. A weaker connectivity is shown with a broken arrow.

connectivities between the methyl groups of each sugar and DNA are shown in Figure 8b. The N,N-dimethylvancosamine is positioned in the minor groove, oriented to the 5' side of the intercalation site and making extensive NOESY contact with 2A, 3T, 8A and 9T. While showing only a weak contact to 5TH4', the H2" proton shows a very strong NOE contact to the H9 proton located on the hedamycin chromophore. Based on this contact, the N,N-dimethylvancosamine is rotated to an orientation below the drug chromophore in the 5' direction. This orientation is further supported by NOE contacts between the drug's H6" and 5TH4', the 2" methyl and 9TH4', and between the 4" methyl and 2AH2, 3TH1', 9TH1' and 9TH5'. Furthermore, the 4" dimethylamino group makes medium to strong contacts to 2AH2, 2AH1', 3TH1', 3TH4' and 8AH2. In contrast, the C8 linked anglosamine orients to the 3' side of the modified guanine, making NOE contact primarily with the 5T, 6A, 7C and 8A residues. The H2' and H6' show strong NOE contacts to 8AH1', the 2' methyl shows NOE contacts to 8AH1', 9TH5'/5" and 9TH4', and the 4' dimethylamino shows strong NOE contacts to 5TH1', 6AH2, 6AH4', 7CH1' and 7CH4'.

NMR-driven molecular modeling

In a 100 ps solvated molecular dynamics simulation using 54 inter-drug–DNA, 76 intra-drug, and 166 intra-DNA constraints for the complete bis-adduct, a molecular model was generated that reflects the NMR results (Fig. 9). In this NMR-derived model of the bis-hedamycin diadduct, the conjugated chromophore stacks between the 3T•8A and the 4G•7C base pairs in roughly a perpendicular orientation to the hydrogen bonds formed by the flanking base pairs. To accommodate this interaction, the DNA has grossly distorted, opening the base pairs to twice the normal distance to allow insertion of the drug chromophore. As predicted from the relatively large upfield shift exhibited by 5TH1', the influence of the C8 aminosugar pulls the

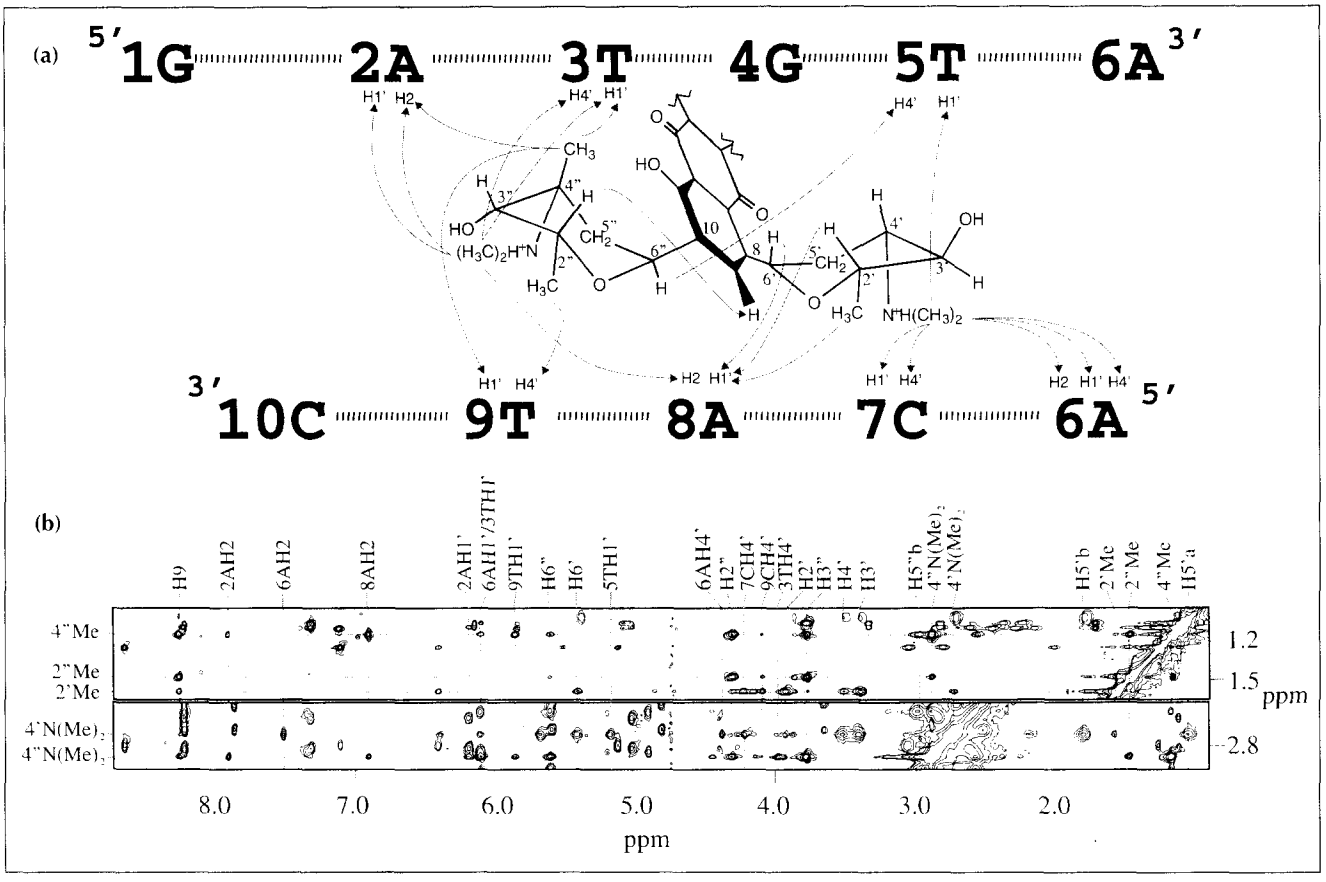

Fig. 8. Summary of key ^{1}H-NOESY connectivities **(a)** and NOESY data (150 ms) **(b)** between hedamycin's C8 and C10 sugar moieties and the DNA minor groove. In (a), NOE connectivities are shown in solid arrows. The NOESY data in (b) shows NOE connectivities of some of the proton and methyl resonances located in the minor groove.

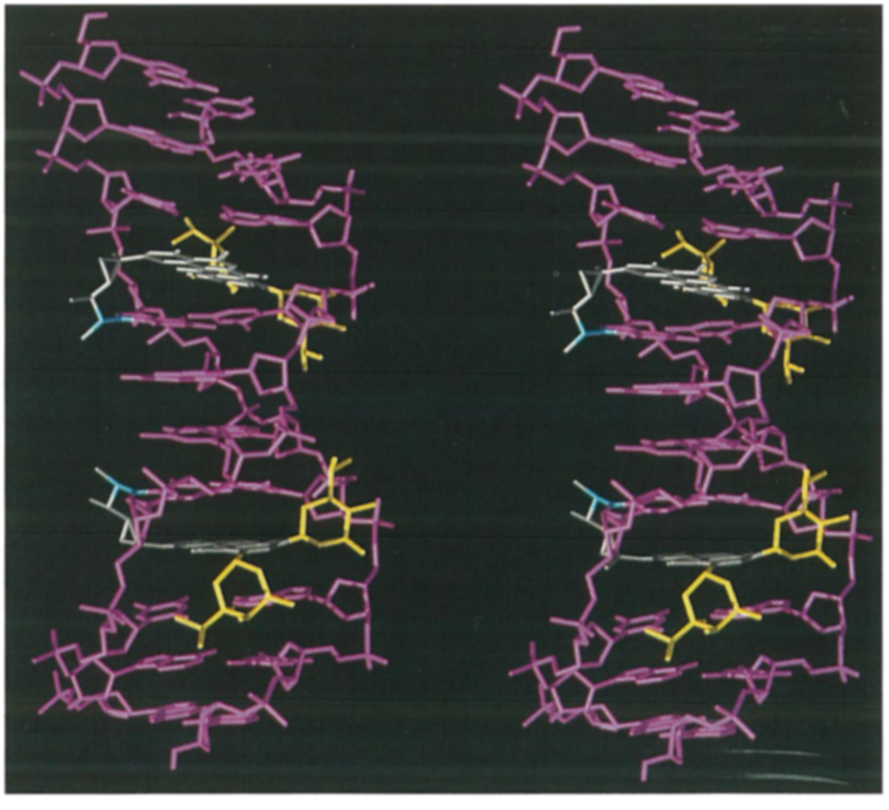

Fig. 9. Stereoview of an NMR-driven molecular model of the bis-hedamycin–10 base-pair DNA duplex adduct. The model depicts intercalation of the drug chromophore into the DNA helix (gray), saccharide binding in the DNA minor groove (yellow) and alkylation at N7 (cyan). The 10 base-pair DNA molecule is rotated so that the major groove faces out at the top of the helix and the minor groove faces out at the bottom of the helix.

tetracyclic chromophore slightly into the minor groove directly under this proton. Despite placing both aminosaccharides into the minor groove, the chromophore remains able to easily span the double helix to covalently attach to N7 of 4G in the major groove.

In the major groove, hedamycin makes the most significant interaction with the DNA molecule, forming a covalent bond through C18 and N7 of 4G. Having a four-carbon span, the C2 epoxide arm easily joins the chromophore to N7 of guanine without causing significant distortion of 4G or the surrounding DNA. Associated with the noncovalently modified strand is the hedamycin 5 methyl, which is pulled in toward the floor of the major groove to make van der Waals contact with the 7CH5 and H6 protons.

Positioned in the minor groove (Fig. 10) are both the C8 linked anglosamine and the C10 linked N,N-dimethylvancosamine moieties. The C10 linked N,N-dimethylvancosamine is directed toward the 5' side of the intercalation site to interact with the covalently modified strand, namely the 3T residue. To the 3' side of the intercalation site, the anglosamine moiety interacts in the minor groove primarily with 7C on the noncovalently modified strand. On the basis of NMR evidence (see Fig. 8), indicating proximity of the dimethylamino in both sugars to the negatively charged O2 carbonyl of each respective pyrimidine, we propose that a key interaction occurs through the formation of a hydrogen bond to the carbonyl, either directly or mediated through a water molecule. Molecular dynamics calculations were performed with direct hydrogen bonding restraints and with hydrogen bonding restraints mediated by a bound water molecule. Both situations satisfied NMR-derived constraints; however, simulations using bound water molecules, similar to those reported in the crystal structure with daunomycin [32], were used to derive the reported structure.

Discussion

Comparison to other pluramycin adducts

Hedamycin interacts with the DNA molecule in a very similar fashion to that reported in previous structural studies involving altromycin B adducted to $[d(GA\underline{AG}^{\star}TACTTC)]_2$ [2] and sapurimycin adducted to $[d(AAT\underline{AG}^{\star}CTATT)]_2$ (C. Lin & D.J. Patel, personal communication). Like the other two pluramycins, hedamycin threads the DNA molecule, covalently attaches to N7 of guanine, and stacks to the 5' side of the modified guanine. Like altromycin B, the C10 linked vancosamine moiety and the closely related C8 linked anglosamine are both positioned in the minor groove.

Subtle structural differences between altromycin B and hedamycin give rise to variations in DNA sequence selectivity and reactivity. Differences in carbohydrate substitution at the C5, C8 and C10 positions of an otherwise similar chromophore appear to modulate alkylation sequence selectivity. Classical pluramycins, characterized by C8 and C10 aminosugar substitutions, demonstrate 5'(Py)G* selectivity, while the altromycins, characterized by a C10 aminodisaccharide and a C5 neutral sugar substitution, demonstrate 5'AG* selectivity [13]. Because both noncovalent analogs, neopluramycin and kidamycin, show only nonspecific DNase I footprinting patterns, and kidamycin shows only nonselective binding to the 10 base-pair DNA duplex in this study, it is probable that sequence selectivity is achieved largely through the covalent alkylation step as opposed to the initial precovalent binding step [13].

Recognition of the minor groove by hedamycin's glycosidic substituents affects the orientation of the intercalating chromophore and, consequently, the proximity of the reactive C2 linked double epoxide to N7 of guanine in the major groove. The hedamycin C8 anglosamine, which is absent in the altromycins, positions to the 3' side of the intercalation site to associate with the noncovalently modified strand, specifically 7C, the cytosine base-paired to the modified guanine. The C10 linked N,N-dimethylvancosamine present in both altromycin B and hedamycin orients to the 5' side of the modified guanine. Although the equivalent C10 sugar in altromycin B also interacts in the minor groove to the 5' side of the intercalation site, the interaction of the N,N-dimethylvancosamine moiety with DNA differs between the two analogs. The hedamycin C10 linked aminosaccharide interacts with the pyrimidine 3T located on the covalently modified strand. This contrasts with the altromycin B aminodisaccharide, in which

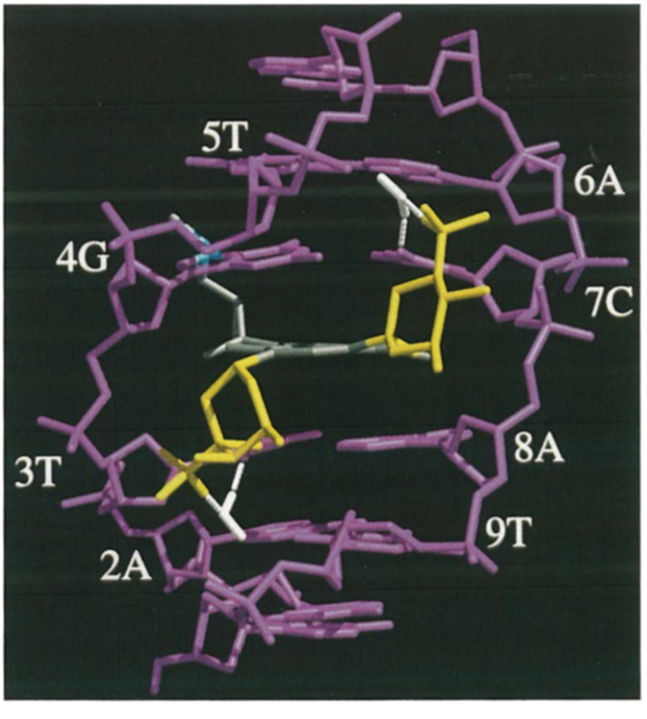

Fig. 10. Molecular representation of the interaction of the hedamycin aminosugars in the minor groove. A water molecule mediating the proposed hydrogen bond between the dimethylamino substituents and the 3TO2 and 7CO2 carbonyls is shown in white.

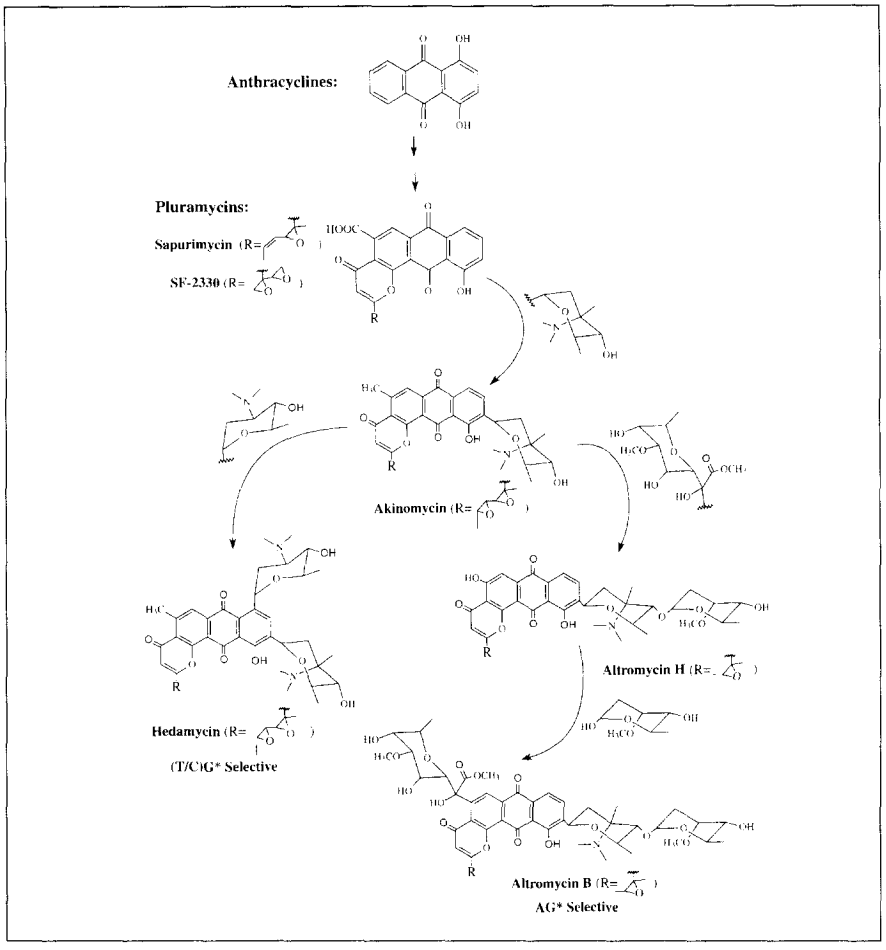

Fig. 11. A proposed evolutionary pathway beginning with the anthracyclines and ending with the most potent compounds from each pluramycin subfamily. The compounds identified as possible intermediates in the evolution pathway were screened for and isolated based on activity and may not fully represent the complete set of compounds in nature.

the C3" linked neutral altrose moiety interacts with the covalently modified strand, while the N,N-dimethylvancosamine interacts primarily with the non-modified strand [2]. A pyrimidine located to the 5' side of the modified guanine, 5'CG★ and 5'TG★, creates a preferred hedamycin alkylation sequence, probably through the interaction of the 4" dimethylamino group and the pyrimidine O2 carbonyl. A purine in the 5' position would require the 4" dimethylamino group to form a less optimal hydrogen bond to the purine N3 position or to create a sterically less favorable hydrogen bond to the carbonyl associated with the base-paired pyrimidine on the non-modified strand. In the case of altromycin B, the reverse situation arises in which the dimethylamino group selects for a pyrimidine located on the non-modified strand, giving rise to the altromycin-preferred sequence 5'AG★ [2,13].

The site of attachment of hedamycin to the DNA molecule also differs from that of other pluramycins studied. While alkylation occurs in a similar fashion through N7 of guanine in all three compounds studied thus far, the hedamycin mechanism of covalent modification occurs through C18 of the terminal epoxide rather than C16 of the proximal epoxide. Attachment to N7 of guanine through C18 of hedamycin then creates a four-carbon link between the tetracyclic chromophore and the modified guanine, as opposed to a two-carbon link in the case of altromycin B and sapurimycin. The bonding geometry of guanine reacted with a C2 single epoxide analog (altromycin B) constrains the modified guanine to tilt in the major groove toward the intercalating chromophore [2,13]. This induced strain is alleviated by the attachment of hedamycin to DNA through a longer, more flexible double epoxide linker. This probably is responsible for the modest gain in both alkylation reactivity and adduct stability demonstrated by hedamycin over altromycin B.

Evolutionary considerations

It is striking that agents have not been discovered that display a combination of glycosidic substitutions drawn from both of the pluramycin subfamilies. Specifically, a compound that bears an aminosaccharide at the C8 position and also has a C5 or C3" altrose substitution has not been reported. The reason for this restricted pattern of glycosidic substitution is probably due to the steric limitations imposed by the DNA helix, which would decrease the ability of the ligand to covalently modify DNA. A hypothetical compound having the C10 aminodisaccharide and a C8 aminosugar would not have room in the minor groove to accommodate both of these substituents. Similarly, an analog possessing a major-groove binding C5 substituent and a minor-groove binding C8 sugar substitution would not easily span the DNA double helix from groove to groove. On the basis of these observations, the evolutionary scheme shown in Figure 11 is proposed for the biosynthesis of the pluramycin class of antibiotics.

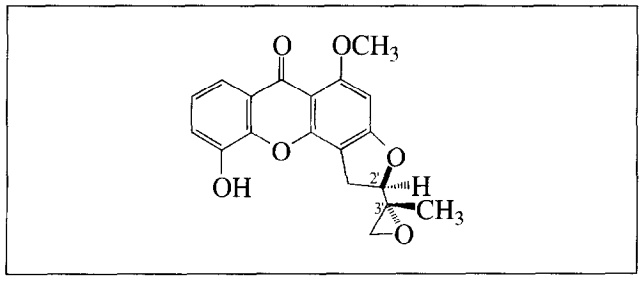

Fig. 12. Chemical structure of the anti-leukemic xanthone psorospermin [36]. Structural analogies to the pluramycin chromophore can be drawn to gain insight into mode of action of these agents.

In light of the structural incompatibilities between subfamilies, the earliest pluramycin antibiotic probably evolved from the anthraquinones, creating a compound very similar to sapurimycin. It is then likely that the antibiotic-producing organism added an N,N-dimethylvancosamine, common to both families, to the C10 position to yield a compound similar to akinomycin, which would probably react equally well with sequences preferred by the classical pluramycins and the altromycins. Divergence occurred at this point, creating two independent families of compounds. The altromycins would be created by adding neutral altroses to the C3" and C5 positions, and the classical pluramycins would be created by attaching an anglosamine sugar moiety to the C8 position. Consequently, the most structurally advanced and biologically potent analogs of each subfamily, altromycin B and hedamycin, have independently evolved from a common ancestor to form the most DNA-reactive compounds of the pluramycin family, each preferentially recognizing mutually exclusive DNA sequence targets.

Comparison of pluramycins to psorospermin

By comparing chemical structure, one can draw several parallels to the anti-leukemic agent psorospermin (Fig. 12) [33]. The psorospermin structure has a dihydrofuranoxanthone skeleton with an attached epoxide that appears to function similarly to that of the pluramycins [34]. The xanthone moiety could intercalate into the DNA molecule, placing the 3,4 benzofuran into the major groove. The epoxide attached through C2 of the benzofuran could then easily alkylate N7 of guanine located in the major groove in a similar fashion to the pluramycins. Due to the R stereochemistry at the C2' position, however, alkylation would be restricted to a guanine residue located to the 5' side of the DNA intercalation site as opposed to the 3' side, as in the case of the pluramycins. *In vivo* studies using psorospermin show that the cytotoxicity of this agent correlates well with the formation of abasic sites and abasic-dependent lesions such as protein–DNA cross-links and DNA strand breaks. This would suggest that the biologically significant DNA lesion would not necessarily be the drug–DNA adduct but the abasic site resulting from drug-induced depurination of the guanine residue. Given the information from this study, design efforts may need to focus on agents that form less stable adducts that readily depurinate. It may also be important to consider the possible role that alkylation to the 5' side of intercalation plays in achieving depurination.

Significance

The structure of the DNA–hedamycin complex determined in these studies, together with the known structure of the DNA–altromycin complex, has yielded an understanding of the carbohydrate-mediated sequence-dependent alkylation displayed by the pluramycin family of DNA interactive agents. Only a few clearly documented examples of carbohydrate-mediated DNA interaction have been described to date. The pluramycins embody three modes of interaction with DNA. First, they have an anthraquinone ring system that intercalates into the DNA. Second, they have an attached aminosugar that binds in the minor groove upon DNA complexation. Third, in conjunction with the basic anthraquinone structure, the pluramycins have evolved a 1,2 pyran ring system upon which they have attached multiple possible epoxide functionalities that can covalently modify DNA through N7 of guanine. In this respect, the pluramycin–DNA lesion is closely analogous to that created by the highly mutagenic DNA intercalator-alkylator aflatoxin [35].

To be effective against tumors *in vivo*, the designed agents should maximize tumor cell-specific cytotoxicity. Selective uptake of a cytotoxic agent at the cellular level would appear to be crucial unless unique intracellular targets can be identified within cancer cells. At the intracellular level, selectivity can be achieved either at the level of DNA sequence or through interaction with pharmacologically selective receptors on or associated with DNA [36]. If ligand-induced mutagenicity and antitumor activity is a function of DNA sequence selectivity, then modification of the glycosidic substitutions at the various corners of the pluramycin chromophore should be able to modulate these biological properties.

Materials and methods

Sample preparations

The self-complementary d(GATGTACATC) DNA strand was synthesized on an automated DNA synthesizer (Applied Biosystems 381A) using the solid phase phosphoramidite method. The DNA synthesis was performed on a 10-μmol scale, leaving the final dimethoxytrityl group on the 5' end of the DNA molecules. The crude sample was deprotected in concentrated NH_4OH at 55 °C overnight and purified by reverse phase chromatography on a C18 column (Dynamax-300A). Purified DNA was then detritylated by dissolving in 80 % acetic acid for 30 min, followed by ether extraction to

remove the acetic acid. The sample was then extensively dialyzed and buffer was adjusted to 10 mM NaH_2PO_4, 100 mM NaCl, 0.5 mM EDTA, pH 6.8.

Hedamycin samples were a gift from the Drug Synthesis and Chemistry Branch, Developmental Therapeutics Program, Division of Cancer Treatment, National Cancer Institute, and were used without further purification. Drug–DNA adduct formation was achieved by adding a 2:1 molar ratio of hedamycin to the purified DNA sample and mixing at 5 °C for several hours. Adduct formation was monitored by one-dimensional NMR until complete alkylation of the DNA had occurred. After addition of drug, the pH was checked and readjusted to pH 6.8. Due to aggregation problems, samples were diluted to 1.0–2.0 mM adduct concentrations and experiments were performed at 30 °C. In between experiments, samples were stored inside NMR tubes at −70 °C to minimize decomposition due to depurination of the hedamycin–guanine adduct.

NMR experiments

All NMR experiments were performed on a Bruker AMX 500 spectrometer in 99.96 % D_2O or 95 % H_2O:5 % D_2O. Phase-sensitive, tppi two-dimensional NOESY, TOCSY and DQF-COSY experiments [27–30] were performed on samples dissolved in D_2O. For these experiments, 1 K data points were acquired in t1 with a spectral width of 5000 Hz. To observe exchangeable protons, a two-dimensional NOESY spectrum was obtained with 150 ms mixing delay in H_2O using a 1–1 echo pulse sequence [37–39] to suppress the water resonance. In this experiment, 1 K of data points were obtained in t1 with a sweep width of 12 000 Hz. Select carbon-13 resonances were identified and characterized using HMQC and HMBC experiments in D_2O [40,41].

Due to a limited sample life, interproton distance constraints were calculated from a single 150 ms NOESY spectrum in D_2O, obtained with 32 scans per increment, 6000 Hz sweep width, and a 5 s relaxation delay between scans. Data was multiplied by a $\pi/2$ shifted sinebell squared window function, zero filled to 2 K and Fourier transformed using Felix 2.0 NMR data processing software. Interproton cross-peaks were integrated and sorted by volume into sixteen distinct bins: four each for proton–proton cross-peaks, methyl–proton cross-peaks, dimethylamino–proton cross-peaks and methyl–dimethylamino cross-peaks, corresponding to very strong, strong, medium and weak connectivities. Upper and lower constraint boundaries were created using the coordinate averages for the protons in the methyl and dimethylaminos. The respective boundaries for each group are: 2.2–3.5, 2.6–4.0, 3.0–4.5, 3.5–5.5; 2.2–3.5, 2.6–4.0, 3.0–5.0, 3.5–6.0; 2.2–4.0, 2.4–4.5, 3.0–6.5, 4.0–7.0; and 4.0–5.0, 4.0–5.5, 5.0–7.0, 5.5–8.0.

Modeling

The SANDER (Simulated Annealing with NMR Driven Energy Restraints) module of AMBER 4.0 [42] was used to perform energy refinement with these NMR-derived distance constraints to derive a model of the hedamycin–d(GATG*TACATC)$_2$ diadduct. The AMBER force field was used with the addition of pseudo energy terms consisting of a flat well potential with parabolic boundaries for each inter-proton connectivity measured. Hedamycin partial atomic charges, calculated by MOPAC 5.0, were incorporated into the force field parameters for electrostatic energy calculations. Additionally, bond, torsion and angle parameters calculated for carbohydrates [43] were included for energy calculations concerning the saccharide moieties in the drug molecule. The N7 of the modified guanine was parameterized assuming planar, sp2 hybridization.

Initial DNA structures were created with the NUCGEN module of AMBER and adjusted in MIDAS [44] to form intercalation sites and to dock the hedamycin molecule. The hedamycin structure was generated by minimizing the reported X-ray structure [20]. The starting structure was then solvated with approximately 600 water molecules, subjected to 30 ps of belly dynamics holding the drug–DNA adduct rigid, minimized, and then slowly heated to 300 K over 10 ps. In the initial period of molecular dynamics, interproton distance constraints were slowly incorporated to 10 kcal mol^{-1} $Å^{-2}$. The system was then maintained at 300 K for 90 ps and minimized *in vacuo*, without constraints, to obtain the reported structure.

Supplementary material available

Included as supplemental material is a list of constraints and final constraint violations.

Acknowledgements: We gratefully acknowledge Steve Sorey, Steve Mizak and Terrence Scahill for NMR technical assistance, NCI for generous gifts of hedamycin, David Bishop for critical reading of the manuscript, and Miguel Salazar and Sean Kerwin for many helpful discussions. Research was supported by The University of Texas at Austin, the Welch Foundation, and the Public Health Service CA-49751 and GM12453-03.

References

1. Sun, D., Hansen, M., Clement, J.J. & Hurley, L.H. (1993). Structure of the altromycin B (N7-guanine) adduct. A proposed prototypic DNA adduct structure for the pluramycin antitumor antibiotics. *Biochemistry* **32**, 8068–8074.
2. Hansen, M. & Hurley, L.H. (1995). Altromycin B threads the DNA helix interacting with both the major and the minor grooves to position itself for site-directed alkylation of guanine N7. *J. Am. Chem. Soc.* **117**, 2421–2429.
3. Uosaki, Y., Yasuzawa, T., Hara, M. & Saitoh, Y. (1991). Sapurimycin, new antitumor antibiotic produced by *Streptomyces*. *J. Antibiot. (Tokyo)* **44**, 40–44.
4. Gonda, S.K., Bryne, K.M., Herver, P.K., Tondeur, Y., Leverato, D. & Hilton, B.D. (1984). Structure and properties of major largomycin FII chromophore components. *J. Antibiot. (Tokyo)* **37**, 1344–1356.
5. Yasuzawa, T., Saitoh, Y. & Sano, H. (1990). Structures of the novel anthraquinone antitumor antibiotics, DC92-B and DC92-D. *J. Antibiot. (Tokyo)* **43**, 485–491.
6. Sequin, U. (1986). The antibiotics of the pluramycin group (4H-anthra[1,2-b]pyran antibiotics. *Fortschr. Chem. Org. Naturst.* **50**, 57–122.
7. Sato, Y., *et al.*, & Kondo, S. (1989). Ankinomycin, a potent antitumor antibiotic. *J. Antibiot. (Tokyo)* **42**, 149–152.
8. Itoh, J., *et al.*, & Kojima, M. (1986). Studies of a new antibiotic SF-2330. *J. Antibiot. (Tokyo)* **39**, 773–779.
9. Nadig, H. & Sequin, U. (1987). Isolation and structure elucidation of some components of the antitumor antibiotic mixture rubiflavin. *Helv. Chim. Acta.* **70**, 1217–1228.
10. Nadig, H., Sequin, U., Bunge, R., Hurley, T., Murphey, D. & French, J. (1985). Isolation and structure of a new antibiotic related to rubiflavin A. *Helv. Chim. Acta.* **68**, 953–957.
11. Abe, N., Enoki, N., Nakakita, Y., Uchida, H., Nakamura, T. & Munekata, M. (1993). Novel antitumor antibiotics, saptoomycins. *J. Antibiot. (Tokyo)* **46**, 1536–1549.
12. Hara, M., Takiguchi, T., Ashizawa, T., Katsushige, G. & Nakano, H. (1991). Sapurimycin, new antitumor antibiotic produced by *Streptomyces*. *J. Antibiot. (Tokyo)* **44**, 33–39.
13. Sun, D., Hansen, M. & Hurley, L.H. (1995). Molecular basis for the DNA sequence specificity of the pluramycins. A novel mechanism involving groove interactions transmitted through the helix via intercalation to achieve sequence selectivity at the covalent bonding step. *J. Am. Chem. Soc.* **117**, 2430–2440.

14. Furukawa, M. & Iitaka, Y. (1980). The structures of kidamycin derivatives: triacetylmethoxykidamycin bis(trimethylammonium) iodide and isokidamycin bis(m-bromobenzoate). *Acta Crystallogr. B* **36**, 2270–2276.
15. Furukawa, M. & Iitaka, Y. (1974). Structure of kidamycin: X-ray analysis of isokidamycin derivatives. *Tetrahedron Lett.* **37**, 3287–3290.
16. Furukawa, M., Hayakawa, I., Ohta, G. & Iitaka, Y. (1975). Structure and chemistry of kidamycin. *Tetrahedron* **31**, 2989–2995.
17. Kondo, S., Miyamoto, M., Naganawa, H., Takeuchi, T. & Umezawa, H. (1977). Structures of pluramycin A and neopluramycin. *J. Antibiot. (Tokyo)* **30**, 1143–1145.
18. Maeda, K., *et al.*, & Umezawa, H. (1956). A new antitumor substance, pluramycin. *J. Antibiot., Ser A.* **9**, 75–81.
19. Byrne, K.M., Gonda, S.K. & Hilton, B.D. (1985). Largomycin FII chromophore component 4, a new pluramycin antibiotic. *J. Antibiot. (Tokyo)* **38**, 1040–1049.
20. Sequin, U.R., Bedford, C.T., Chung, S.K. & Scott, A.I. (1977). The structure of the antibiotic hedamycin. I. Chemical, physical, and spectral properties. *Helv. Chim. Acta* **60**, 896–906.
21. Zehnder, M., Sequin, U. & Nadig, H. (1979). The structure of the antibiotic hedamycin. V. Crystal structure and absolute configuration. *Helv. Chim. Acta* **62**, 2525–2533.
22. Sequin, U. (1978). The structure of the antibiotic hedamycin. II. Comparison of hedamycin and kidamycin. *Tetrahedron* **34**, 761–767.
23. Brill, G.B., McAlpine, J.B., Whittern, D.N. & Buko, A.M. (1990). Altromycins, novel pluramycin-like antibiotics. II. Isolation and elucidation of structure. *J. Antibiot. (Tokyo)* **43**, 229–237.
24. McAlpine, J.B., *et al.*, & Burres, N.S. (1994). Altromycins: a new family of antitumor antibiotics — discovery and biological evaluation. In *Antitumor Drug Discovery and Development.* (Valeriote, F.A., Corbett, T.H. & Baker, L.H., eds), pp. 95–117, Kluwer Academic Publishers, Boston.
25. Jackson, M., *et al.*, & McAlpine, J.B. (1990). Altromycins, novel pluramycin-like antibiotics. I. Taxonomy of the producing organism, fermentation and antibacterial activity. *J. Antibiot. (Tokyo)* **43**, 223–228.
26. Gopalakrishnan, S., Harris, T.M. & Stone, M.P. (1990). Intercalation of aflatoxin B_1 in two oligonucleotide adducts: comparative ^{1}H NMR analysis of d(ATC^{AFB}GAT)·d(ATCGAT) and d(AT^{AFB}GCAT)$_2$. *Biochemistry* **29**, 10438–10448.
27. Bax, A. & Davis, D. (1985). Practical aspects of two-dimensional transverse NOE spectroscopy. *J. Magn. Reson.* **63**, 207–213.
28. Bax, A. & Davis, D.G. (1985). MLEV-17-based two-dimensional homonuclear magnetization transfer spectroscopy. *J. Magn. Reson.* **65**, 355–360.
29. Drobny, G., Pines, A., Sinton, S., Weitekamp, D.P. & Wemmer, D. (1987). Fourier transform multiple quantum nuclear magnetic resonance. *Faraday Symp. Chem. Soc.* No. 12, 49–55.
30. Shaka, A. & Freeman, R. (1983). Simplification of NMR spectra by filtration through multiple-quantum coherence. *J. Magn. Reson.* **51**, 169–173.
31. Hare, D.R., Wemmer, D.E., Chou, S.H., Drobny, G. & Reid, B.R. (1983). Assignment of the non-exchangeable proton resonances of d(CGCGAATTCGCG) using two-dimensional nuclear magnetic resonance methods. *J. Mol. Biol.* **171**, 319–336.
32. Nunn, C., Meervelt, L., Zhang, S., Moore, M. & Kennard, O. (1991). The crystal structures of d(TGTACA) and d(TGATCA) complexed with daunomycin. *J. Mol. Biol.* **222**, 167–177.
33. Habib, A., *et al.*, & Cassady, J. (1987). Structure and stereochemistry of psorospermin and related cytotoxic dihydrofuranoxanthones from *Psorospermum febrifugum*. *J. Org. Chem.* **52**, 412–418.
34. Permana, P., Ho, D., Cassady, J. & Snapka, R. (1994). Mechanism of action of the antileukemic xanthone psorospermin: DNA strand breaks, abasic sites, and protein–DNA cross-links. *Cancer Res.* **54**, 3191–3195.
35. McConnell, I.R. & Garner, R.C. (1994). DNA adducts of aflatoxins, sterigmatocystin and other mycotoxins. In *DNA Adducts: Identification and Biological Significance.* (Hemminki, K., Dipple, A., Shuker, D.E.G., Kadlubar, F.F., Segerbäck, D. & Bartsch, H., eds), pp. 45–89, IARC Scientific Publications, No.125, Lyon.
36. Hurley, L.H. (1989). DNA and associated targets for drug design. *J. Med. Chem.* **32**, 2027–2033.
37. Plateau, P. & Gueron, M. (1982). Exchangeable proton NMR without base-line distortion, using new strong-pulse sequences. *J. Am. Chem. Soc.* **104**, 7310–7311.
38. Sklenar, B. & Bax, A., (1987). Spin-echo water suppression for the generation of pure-phase two dimensional NMR spectra. *J. Magn. Reson.* **74**, 469–479.
39. Blake, P. & Summers, M. (1990). Noesy-1-1-echo spectroscopy with eliminated radiation damping. *J. Magn. Reson.* **86**, 622–625.
40. Bax, A. & Summers, F. (1986). ^{1}H and ^{13}C assignments from sensitivity enhanced detection of heteronuclear multiple-bond connectivity by 2D multiple quantum NMR. *J. Am. Chem. Soc.* **108**, 2093–2094.
41. Bax, A., Griffey, H. & Hawkins, B. (1983). Correlation of proton and nitrogen-15 chemical shifts by multiple quantum NMR. *J. Magn. Reson.* **55**, 301–315.
42. Pearlman, D.A., *et al.*, & Kollman, P.A. (1991). *Amber 4.0.* University of California, San Francisco.
43. Homans, S.W. (1990). A molecular mechanical force field for the conformational analysis of oligosaccharides: comparison of theoretical and crystal structures of Manα1–3Manβ1–4GlcNAc. *Biochemistry* **29**, 9110–9118.
44. Ferrin, T.E., Huang, C.C., Jarvis, L.E. & Langride, R. (1988). The MIDAS display system. *J. Mol. Graphics* **6**, 13–37.

Received: **17 Mar 1995**; revisions requested: **6 Apr 1995**; revisions received: **10 Apr 1995**. Accepted: **10 Apr 1995**.